Published in final edited form as:
Nucl Med Biol. 2009 August ; 36(6): 651–658. doi:10.1016/j.nucmedbio.2009.03.008.

Comparison of radiolabeled isatin analogs for imaging apoptosis with positron emission tomography

Delphine L. Chen, M.D.[1], **Dong Zhou, Ph.D.**[1], **Wenhua Chu, Ph.D.**[1], **Phillip E. Herrbrich, B.S.**[1], **Lynne A. Jones, B.S.**[1], **Justin M Rothfuss, B.S.**[1], **Jacquelyn T. Engle, B.S.**[1], **Marco Geraci, Ph.D.**[2], **Michael J. Welch, Ph.D.**[1], and **Robert H. Mach, Ph.D.**[1]

[1]Mallinckrodt Institute of Radiology, Washington University School of Medicine, St. Louis, MO.

[2]Faculty of Medical and Human Sciences, University of Manchester, Manchester, United Kingdom.

Abstract

Introduction—Caspase-3 is one of the executioner caspases activated as a result of apoptosis. Radiolabeled isatins bind to caspase-3 with high affinity and are potential tracers for use with positron emission tomography to image apoptosis. We compared the ability of 2 novel radiolabeled isatins, [^{18}F]WC-IV-3 and [^{11}C]WC-98, to detect caspase-3 activation in a rat model of cycloheximide-induced liver injury.

Methods—Male Sprague-Dawley rats were treated with cycloheximide and then imaged with microPET 3 hours later with [^{18}F]WC-IV-3 and [^{11}C]WC-98. Biodistribution studies were also performed simultaneously, with caspase-3 activation verified by fluorometric enzyme assay and Western blots.

Results—MicroPET imaging studies demonstrated similar behavior of both tracers but with a lower maximum peak with [^{11}C]WC-98 than with [^{18}F]WC-IV-3. Biodistribution studies demonstrated increased uptake of both tracers in the liver and spleen, but this was statistically significant only in the liver with both compounds. The level of [^{18}F]WC-IV-3 uptake appeared to correlate roughly with rates of caspase-3 activation by the enzyme assay, but the magnitude of difference between treated and control groups was lower than that observed in previously published data with [^{18}F]WC-II-89, another radiolabeled isatin analog. Activation was also confirmed in the liver and spleen but not in fat by Western blot.

Conclusion—[^{18}F]WC-IV-3 uptake appears to correlate with increased caspase-3 enzyme activity, but the dynamic range of uptake of these 2 tracers appears to be less than that seen with [^{18}F]WC-II-89. Studies are ongoing to verify these results in other animal models of apoptosis.

Keywords

apoptosis; caspase-3; positron emission tomography; radiolabeled isatins; liver injury

Corresponding Author: Delphine L. Chen, MD, Division of Nuclear Medicine, Mallinckrodt Institute of Radiology, Washington University School of Medicine, Campus Box 8223, 510 S. Kingshighway Blvd., St. Louis, MO 63110.

Introduction

Apoptosis, or programmed cell death, is a highly conserved mechanism of cell death that is required for the normal maintenance of healthy tissues. However, dysregulation of the apoptotic pathways has been implicated in a number of diseases, including oncologic, cardiovascular, immunologic, neurodegenerative, and pulmonary diseases.[1–5] Novel drug therapies targeting the apoptotic pathways that can modulate the pathophysiology of these diseases are currently being investigated.[6,7] Therefore, the development of non-invasive imaging methods that can quantify the level of apoptosis in patients and detect changes in these levels as a result of apoptosis-targeted therapies would be highly useful for the drug development process and potentially for the clinical assessment of these conditions.

Positron emission tomography (PET) is an imaging modality that easily lends itself to such an application. PET is highly sensitive, requiring only nanomolar or femtomolar concentrations of tracer to generate an adequate signal, and therefore is also very safe because tracer amounts of mass can be injected to achieve interpretable images. Accurate quantification of the signal can also be readily achieved due to coincidence detection of the annihilation photons generated from decay of the positron-emitting isotope.

The apoptotic cell death pathways require the activation of cysteine aspartyl-specific proteases, or caspases.[6,8,9] Caspase activation has been identified as a specific hallmark of apoptotic activation which is required to develop typical apoptotic cellular morphology changes, as treatment with pan-caspase inhibitors can block the progression of apoptosis and divert cells into cell death by necrosis.[10–12] Two classically described pathways, the mitochondrial or "intrinsic" and death receptor or "extrinsic" pathways,[13] both lead to activation of the downstream effector caspase 3.[8,12,14] Therefore, methods for non-invasively assessing active caspase-3 enzyme activity in principle should be useful in distinguishing apoptotic from necrotic cells in vivo.

The isatins are potent, competitive reversible inhibitors of caspase-3.[15,16] We have recently reported the synthesis of a panel of these compounds that can be radiolabeled with F-18 or C-11 for use as PET tracers for imaging caspase-3 activation. We have also evaluated one F-18 isatin analog in the rat model of cycloheximide-induced liver injury.[17] Faust and colleagues have also evaluated another F-18 labeled isatin in a mouse model of cardiac ischemia-reperfusion.[18] The purpose of this study was to compare two additional radiolabeled isatin analogs, the pyrrolidine analog [^{11}C]WC-98 and the azetidine analog [^{18}F]WC-IV-3, with our previously published data with [^{18}F]WC-II-89 in the rat model of cycloheximide-induced liver apoptosis, to compare their effectiveness in imaging caspase-3 activation in vivo.

Materials and Methods

Synthesis of [^{18}F]WC-IV-3 and [^{11}C]WC-98

[^{18}F]WC-IV-3 was synthesized from a mesylate precursor via a nucleophilic substitution using [^{18}F]fluoride/Kryptofix 2.2.2. complex, followed by hydrolysis using 1 N HCl. The specific activity was determined to be $8.9\times10^4 \pm 5.4\times10^4$ GBq/mmol (2415 ± 1463 Ci/mmol) (n = 2). [^{11}C]WC-98 was synthesized via a O-methylation of a precursor using [^{11}C]CH_3I in high yields with high chemical and radiochemical purities. [^{11}C]WC-98 and [^{18}F]WC-IV-3 were confirmed by coelution with the corresponding nonradioactive standard WC-IV-3 and WC-98 on an analytical HPLC system.

Synthesis of isatin sulfonamide [^{18}F]WC-IV-3—Synthesis is summarized in Scheme 1. 100 mCi [^{18}F]fluoride in *ca* 200 μL 0.2 N K_2CO_3 solution was dried in the presence of Kryptofix 2.2.2. (10 mg) and K_2CO_3 (1.8 mg) in a 10 mL Pyrex tube by azeotropic distillation

with CH_3CN (3 × 1 mL) at 110 °C under nitrogen flow, then a solution of WC-IV-3 mesylate precursor (1.1 mg, 1.83 μmol) in anhydrous DMSO (600 μL) was added into the Pyrex tube, which was then capped firmly. The reaction mixture was shaken well and was heated by microwave irradiation (60W) for 30 and 25 sec with an interval of 1 min between them. Then 1 N HCl (500 μL) was added and the mixture in the capped tube was heated by microwave irradiation (60W) for 25 sec. The reaction mixture was diluted in water (40 mL) and then passed through a Waters classic C18 Sep-Pak cartridge to trap the product, which was eluted by back-flushing with CH_3CN (1.0 mL), MeOH (1.0 mL) and water (2.0 mL) for HPLC injection. The purification was carried out by a semipreparative HPLC system (Alltech Econosil C18 250 × 10 mm 10μ) eluting with 20% acetonitrile, 45% methanol and 35% 0.1 M ammonium formate buffer (pH=4.5) at a flow rate of 4 mL/min and UV at 251 nm. The radioactive peak corresponding to [^{18}F]WC-IV-3 was detected at 18 to 20 min by the radioactivity detector and was collected (0.5 min per tube). The majority of the collected activity (mainly in 4 tubes) was diluted in water (30 mL), then a C18 Sep-Pak was used to extract the activity and the Sep-Pak was washed with water (10 mL) to remove any trace of CH_3CN. [^{18}F]WC-IV-3 was eluted by back-flushing with ethanol in a portion of 0.5mL. The portion containing the majority of the activity (less than 2 mL) was used for the final dose preparation (10% ethanol, 90% saline). The isolated yield (without decay correction) was 24.1 ± 0.4 % (n = 2) with a radiochemical purity of > 99% and specific activity of 2415 ± 1463 (n = 2) at the end of synthesis. The total synthesis time was *ca* 90 min.

Synthesis of isatin sulfonamide [^{11}C]WC-98—Into a solution of WC-98 precursor (0.2 mg, 0.41 μmol) in CH_3CN (100 μL) was added 1N Bu_4NOH/H_2O (0.83 μL, 0.83 μmol) in CH_3CN (100 μL). The mixture was vortexed and cooled down to 0 °C. After [^{11}C]CH_3I was trapped by bubbling the activity through the solution at 0 °C, the reaction mixture was sealed and heated at 88 °C for 4 min, then 88 °C for 4 min after the addition of 1N HCl (200 μL). Finally the reaction mixture was diluted with HPLC solvent (1.5 mL) for HPLC injection. [^{11}C]WC-98 was purified by a reverse phase HPLC system (Alltech Econosil C18 250 × 10 mm 10μ) eluting with 25% CH_3CN, 25% 0.1 M ammonium formate buffer (pH = 4.5) and 50% MeOH with UV at 237 nm and a flow rate at 4 mL/min. The corresponding radioactivity for [^{11}C]WC-98 at 11–13 min of HPLC elution was diluted in water (150 mL), and extracted in a Water classic C18 Sep-Pak by passing the diluted solution through it. After the Sep-Pak was washed with water (10 mL), [^{11}C]WC-98 was eluted from the Sep-Pak with ethanol (1.5 mL). The final doses for subsequent studies were prepared in 10% ethanol/90% saline. The radiochemical purity of isatin [^{11}C]WC-98 was determined by an analytical HPLC (Alltech Altima C18 250 × 4.6 mm 10μ), eluted with 75% methanol and 25% 0.1 M ammonium formate buffer (pH = 4.5) at a flow rate of 1.5 mL/min and UV at 251 nm. [^{11}C]WC-98 was eluted at 6.5 min and confirmed by co-elution with the nonradioactive standard WC-98 on the analytical HPLC system. By comparison of the integrated sample UV signal with a calibrated compound mass/UV absorbance curve, the specific activity was determined at the end of synthesis. [^{11}C] WC-98 was synthesized in 61 ± 11% (n = 4) yield (decay corrected) in *ca* 60 minutes with the radiochemical purity of > 99% and a specific activity of 707 ±110 Ci/mmol (n = 4), determined at the end of synthesis.[19]

Analysis of Specificity and Chemical Characteristics

Specificity of both compounds for caspase-3 was determined using enzyme inhibition assays to determine the IC_{50} values for caspases 1, 3, 6, 7, and 8 as previously described.[17] Approximate log P values were calculated using ACD/Labs 7.0 (Toronto, Ontario, Canada).

Animal Preparation and Experimental Groups

The protocol for these studies was reviewed and approved by the Animal Studies Committee at Washington University School of Medicine. The cycloheximide model of liver apoptosis in

the rat has been used to study hepatocyte apoptosis, with no evidence of necrosis in the liver when cycloheximide is given at low doses.[20,21] Male Sprague-Dawley rats, 222 ± 6 g (7.4 weeks old) and 298 ± 10 g (9 weeks old) for the [^{18}F]WC-IV-3 and [^{11}C]WC-98 studies respectively, were briefly anesthetized with isoflurane 1–2% and then injected i.v. with 5 mg/kg of cycloheximide (Sigma-Aldrich, St. Louis, MO) 3 hours prior to tracer injection. Animals were allowed to recover and then reanesthetized with isoflurane 1–2% for microPET imaging and prior to euthanization for the biodistribution study.

Biodistribution Study

A biodistribution study was performed to determine changes in tracer uptake levels over time. Animals were divided into treated and untreated control groups, with N = 4 in each group at each time point. Rats were sacrificed at 5 min, 30 min and 1 h after injection of ~31 μCi of [^{18}F]WC-IV-3, and at 5 min and 30 min after injection of ~38 μCi of [^{11}C]WC-98 (both tracers administered in 100 μl of 15% ethanol/normal saline). Tracer doses were drawn and counted at the beginning of and then injected into each animal over the course of the experiment so that the same mass of compound was injected into each animal. Injection syringes were post-counted and decay-correction applied to determine the injected dose. After sacrifice, the following organs were harvested: blood, lungs, heart, thymus, liver, spleen, kidney, brain, fat, muscle, bone, tail. Fewer organs were taken for the C-11 study due to the shorter half-life of the isotope. Organs were blotted to remove excess blood and then weighed and counted separately in a gamma counter. The percent injected dose per gram of tissue (%ID/g) was determined for each organ. Any animal with 10% or more of the injected dose in the tail was excluded from the analysis.

MicroPET Imaging Acquisition and Data Analysis

Treated and control animals were imaged using a Siemens/CTI Focus 120 and Focus 220 microPET scanner (Concord, KY). A dynamic 60-minute acquisition was performed after injection of ~250 μCi of [^{18}F]WC-IV-3 or ~340 μCi of [^{11}C]WC-98 (again with both tracers in 15% ethanol/normal saline) using the following framing schedule: 24 × 5 sec, 8 × 60 sec, 6 × 180 sec, 4 × 300 sec. Images were reconstructed using filtered back-projection. Volumes of interest were placed over the liver to generate time-activity curves.

Caspase-3 Determination by Fluorometric Enzyme Assay and Western Blotting

Caspase-3 activation was determined by fluorometric caspase-3 assay and Western blotting in liver and spleen samples taken directly from the biodistribution study performed with [^{18}F]WC-IV-3. A separate experiment was also performed in rats under the same conditions as the biodistribution studies in which the liver, spleen, muscle, and fat were taken and Western blots were performed to assess for caspase-3 activation. The organ of interest was homogenized on ice in extraction buffer for protein extraction according to a previously described protocol.[22]

Fluorometric analysis was performed according to a previously published protocol.[22] Briefly, 200 μg of protein were incubated in assay buffer with 20 μM of Ac-DEVD-AMC substrate (Biomol International, LP, Plymouth Meeting, PA) +/− 1 μM of the caspase-3 inhibitor Ac-DEVD-CHO (Sigma-Aldrich, St. Louis, MO). Fluorescence was measured every 15 min over 4 h and plotted over time. The rate of caspase-3 activity (units/min/μg protein) was then calculated from the slope of the linear portion of the curve (generally taken from the first 1–2 h of time points measured).

For the Western blots, 100 μg of protein were loaded into each lane of a 4–15% Tris-HCl gel and run in running buffer for ~60–90 min at 100 volts. Protein was transferred to an Immobilon P membrane (Millipore, Inc.) on ice. The membrane was then blocked with 5% milk in tris-buffered saline, blotted overnight with primary antibody for caspase-3 at 1:1000 dilution,

washed, blotted with a peroxidase-conjugated secondary antibody, and then washed again before developing with a chemiluminescent developing solution (SuperSignal West Pico Chemiluminescent Substrate, Thermo Scientific).

Statistical analyses

Statistical analysis was performed on data obtained from the biodistribution studies. Data is represented as the mean ± standard deviation (SD) except for the 5 min treated group from the biodistribution study for [^{11}C]WC-98 as N = 2 for this group due to bad tracer injections. The average uptake of different organs in treated animals was compared to controls at each time point for the biodistribution study using a Student's t-test with a stepdown Bonferroni correction to account for multiple organ comparisons.[23] All analyses were run with SAS 9.1 (SAS Institute Inc., Cary, NC).

Results

The structures of [^{18}F]WC-IV-3 and [^{11}C]WC-98 are shown in Figure 1. The inhibitory effect of these compounds on various caspases is shown in Table 1. The specific activity of [^{18}F]WC-IV-3 was 2280 Ci/mmol and of [^{11}C]WC-98 was 1400 Ci/mmol for these experiments. MicroPET imaging demonstrated increased uptake in the liver with both tracers (Figure 2), with time-activity curves similar in shape to that seen with [^{18}F]WC-II-89 (Figure 3). However, the peak uptake of [^{11}C]WC-98 in both treated and control animals was less than that seen with [^{18}F]WC-IV-3. The peak of tracer uptake with [^{18}F]WC-IV-3 was comparable to that observed with [^{18}F]WC-II-89. Graphs of the change in ratio of uptake in treated to control animals over time demonstrate that the differences in uptake with [^{18}F]WC-IV-3 persist over the imaging period, whereas these difference decrease over time with [^{11}C]WC-98.

The results from the biodistribution studies are shown in Table 2 and Table 3. Increased [^{18}F]WC-IV-3 activity was observed in multiple organs at 30 min after tracer injection. While these differences persisted at 1 h, they were not statistically significant except in the liver (Table 2). The differences observed in fat at 30 min with [^{11}C]WC-98 and at 1 h with [^{18}F]WC-IV-3 show that the uptake of the tracer was higher in the control animals, therefore indicating that there is no specific uptake in the fat as a result of the cycloheximide injury. Comparison of the relative increases in uptake with [^{18}F]WC-IV-3 and [^{11}C]WC-98 at 30 min and with [^{18}F]WC-IV-3 and [^{18}F]WC-II-89 at 1 hour are shown in Figure 4. As with the time-activity curves, there is clearly higher uptake in the liver with [^{18}F]WC-IV-3 compared to [^{11}C]WC-98; however, the differences in splenic uptake are comparable between the two radiotracers at 30 min (Figure 4A). The differences in relative splenic uptake with [^{18}F]WC-IV-3 and [^{18}F]WC-II-89 are more striking, with clearly more marked uptake of [^{18}F]WC-II-89 at 1 h (Figure 4B).

Fluorometric assay of the liver and spleen samples taken from the [^{18}F]WC-IV-3 biodistribution demonstrated increased caspase-3 activity in the treated groups compared with controls (Figure 5). The relative differences in the levels of uptake of [^{18}F]WC-IV-3 in both liver and spleen appear to correlate with the relative differences in measured caspase-3 enzyme activity. Western blots of various organs from the same study also demonstrated caspase-3 activation in both liver and spleen. Figure 6 illustrates representative Western blots from the animals sacrificed at 30 minutes. Similar results were noted in the animals sacrificed at 5 minutes and 1 hour. A separate study in animals sacrificed at a time point equivalent to the 5-minute animals in the biodistribution study demonstrated similar findings in the liver and spleen as that shown in Figure 6 but no caspase-3 activation in muscle or fat (data not shown).

Discussion

The development of imaging agents for imaging apoptosis to date has been limited by non-specificity of the available tracers for the apoptotic cell death pathways. Radiolabeled annexin V analogs will bind to phosphatidyl serine residues that are exposed in apoptotic cells via externalization of the residues and in necrotic cells due to the loss of cell membrane integrity that accompanies necrosis.[24,25] Another group of small molecules, dansyl derivatives, have been shown to enter apoptotic cells and have been labeled with F-18 for apoptosis imaging, although in vivo biologic imaging has not yet been reported.[26] However, the mechanism by which this occurs is not well-defined, and studies to date have not demonstrated that these compounds can differentiate apoptotic cells specifically from a mixed apoptotic/necrotic cell population. Therefore, the development of tracers that can differentiate apoptotic from necrotic cells in vivo would be highly useful in non-invasively assessing the level of apoptosis, whether as a marker for the severity of a particular disease or as a method of assessing response to therapies targeting the apoptotic pathways.

The caspase-3 enzyme is an attractive target for this purpose, as the classic apoptotic pathways converge on activation of this effector enzyme.[1] We previously demonstrated that [^{18}F]WC-II-89, a pyrrolidine-sulfonamide isatin analog, binds to caspase-3 in the liver and spleen after administration of cycloheximide in rats.[17] In this study, we evaluated two additional radiolabeled isatin analogs, [^{18}F]WC-IV-3 (an azetidine-sulfonamide analog) and [^{11}C]WC-98 (another pyrrolidine-sulfonamide analog), both with affinities for caspase-3 that are similar to [^{18}F]WC-II-89 (Table 1). While an F-18 tracer is advantageous given the longer half-life of F-18, a C-11-labeled tracer can be highly useful in multiple tracer studies, particularly if used in conjunction with other tracers that interrogate either other cell death pathways or more proximal enzyme targets in the apoptotic cascade. The biodistribution studies demonstrated that, in the control animals, both analogs behaved similarly to [^{18}F]WC-II-89, with rapid clearance of activity from the blood and normal excretion via the hepatobiliary and, to a lesser extent, renal systems (Table 2 and Table 3).

While hepatobiliary excretion of these compounds may limit the usefulness of evaluating uptake in the liver as a measure of the efficacy of these tracers to bind to caspase-3, it is still clear from the time-activity curves that there is continued excretion of the tracer over time. This suggests that binding of the tracer to caspase-3 in the liver may contribute to the increased retention and that hepatocyte dysfunction may not be the sole explanation for this pattern. This will be evaluated in future studies using tracers that are also excreted by the liver but do not bind specifically to caspase-3.

We can also draw conclusions about these tracers by looking at organs other than the liver and kidneys. For this reason, we chose to evaluate the spleen, as it was quite sensitive to caspase-3 activation by cycloheximide administration, based on our fluorometric assay results (Figure 5). Both [^{18}F]WC-IV-3 and [^{11}C]WC-98 levels appear to track with levels of caspase-3 activation as measured by the fluorometric assay (Figure 5). However, in this study, the dynamic range of tracer uptake did not appear to be as wide as that seen with the fluorometric assay. Our previously published results demonstrated an almost 200% increase in [^{18}F]WC-II-89 uptake in spleens from treated animals over that seen in controls.[17] These findings suggest that [^{18}F]WC-IV-3 and [^{11}C]WC-98 may not discriminate between varying caspase-3 levels in vivo as well as [^{18}F]WC-II-89.

It is not clear why the performance of these tracers with similar potencies for inhibiting caspase-3 and slightly lower log P values than [^{18}F]WC-II-89 (see Table 1) would differ as much as we have observed. Both of these compounds were less lipophilic than [^{18}F]WC-II-89 and did not adsorb to glass or plastic nearly to the extent [^{18}F]WC-II-89 did; however, we

chose to use a 15% ethanol/saline solution to administer both compounds as we found this to be the optimal solvent for administering [^{18}F]WC-II-89 to minimize adsorption to the injection syringes. Also, while we did not evaluate specifically the metabolism of these tracers in vivo, the distribution kinetics of both tracers in the dynamic microPET imaging studies were very similar to that observed with [^{18}F]WC-II-89. Therefore, we did not feel that these factors could adequately explain the findings in this study.

One possible explanation for these less dramatic differences in liver uptake of [^{11}C]WC-98 and splenic uptake of [^{18}F]WC-IV-3 is variability in the animals' responses to cycloheximide. The animals used for the [^{18}F]WC-IV-3 study were smaller and slightly younger than the ones used for the [^{11}C]WC-98 study. While the slight weight and age difference between the groups would not be expected to result in dramatic differences in apoptotic activation, especially since we titrated the dose of cycloheximide to weight, it cannot be excluded. Additionally, the model induces mild hepatic injury from which the rats can recover; therefore, at these lower apoptotic levels, the levels of caspase-3 may be more variable. In the current study, we demonstrated with both the quantitative fluorometric caspase-3 enzyme assay and Western blots that the levels of caspase-3 activation can vary widely in the cycloheximide model of apoptosis. Our data also suggest a threshold of caspase-3 activation may be required for these compounds to be able to detect the change in vivo. Therefore, we plan to evaluate other models of apoptosis to further evaluate the efficacy of these tracers, particularly in clinically relevant models to determine whether these tracers can indeed be used to image the levels of apoptosis one would expect in a clinical scenario (e.g. evaluating tumor cell apoptosis in response to chemotherapy treatment). These studies are ongoing.

Conclusions

The in vivo uptake of the azetidine-sulfonamide isatin analog [^{18}F]WC-IV-3 appears to correlate with the rate of caspase-3 activation in various organs, but neither [^{18}F]WC-IV-3 nor [^{11}C]WC-98 appear to discriminate as well between varying levels of caspase-3 activation as [^{18}F]WC-II-89 in the rat model of cycloheximide-induced liver injury. Studies are ongoing to compare the behavior of these tracers in other models of apoptosis to confirm these initial findings.

References

1. Mach, RH. Functional imaging of cellular death. In: Schuster, DP.; Blackwell, TJ., editors. Molecular Imaging of the Lungs. Boca Raton: Taylor and Francis Group; 2005. p. 327-348.
2. Yanga Q, Underwooda MJ, Hsina MK, Liub XC, He GW. Dysfunction of pulmonary vascular endothelium in chronic obstructive pulmonary disease: basic considerations for future drug development. Curr Drug Metab 2008;9(7):661–667. [PubMed: 18781916]
3. Aneja A, Tang WH, Bansilal S, Garcia MJ, Farkouh ME. Diabetic cardiomyopathy: insights into pathogenesis, diagnostic challenges, and therapeutic options. Am J Med 2008;121(9):748–757. [PubMed: 18724960]
4. Cook MC. B cell biology, apoptosis, and autoantibodies to phospholipids. Thromb Res 2004;114(5–6):307–319. [PubMed: 15507260]
5. Friedlander RM. Apoptosis and caspases in neurodegenerative diseases. N Engl J Med 2003;348(14):1365–1375. [PubMed: 12672865]
6. Reed JC. Apoptosis mechanisms: implications for cancer drug discovery. Oncology (Williston Park) 2004;18(13 Suppl 10):11–20. [PubMed: 15651172]
7. Zeitlin BD, Zeitlin IJ, Nor JE. Expanding circle of inhibition: small-molecule inhibitors of Bcl-2 as anticancer cell and antiangiogenic agents. J Clin Oncol 2008;26(25):4180–4188. [PubMed: 18757333]
8. Green DR. Apoptotic pathways: ten minutes to dead. Cell 2005;121(5):671–674. [PubMed: 15935754]

9. Thornberry NA, Lazebnik Y. Caspases: enemies within. Science 1998;281(5381):1312–1316. [PubMed: 9721091]
10. Broker LE, Kruyt FA, Giaccone G. Cell death independent of caspases: a review. Clin Cancer Res 2005;11(9):3155–3162. [PubMed: 15867207]
11. Kitanaka C, Kuchino Y. Caspase-independent programmed cell death with necrotic morphology. Cell Death Differ 1999;6(6):508–515. [PubMed: 10381653]
12. Salvesen GS, Dixit VM. Caspases: intracellular signaling by proteolysis. Cell 1997;91(4):443–446. [PubMed: 9390553]
13. Vaux DL, Strasser A. The molecular biology of apoptosis. Proc Natl Acad Sci U S A 1996;93(6): 2239–2244. [PubMed: 8637856]
14. Elmore S. Apoptosis: a review of programmed cell death. Toxicol Pathol 2007;35(4):495–516. [PubMed: 17562483]
15. Chapman JG, Magee WP, Stukenbrok HA, Beckius GE, Milici AJ, Tracey WR. A novel nonpeptidic caspase-3/7 inhibitor, (S)-(+)-5-[1-(2-methoxymethylpyrrolidinyl)sulfonyl]isatin reduces myocardial ischemic injury. Eur J Pharmacol 2002;456(1–3):59–68. [PubMed: 12450570]
16. Lee D, Long SA, Adams JL, Chan G, Vaidya KS, Francis TA, Kikly K, Winkler JD, Sung CM, Debouck C, Richardson S, Levy MA, DeWolf WE Jr, Keller PM, Tomaszek T, Head MS, Ryan MD, Haltiwanger RC, Liang PH, Janson CA, McDevitt PJ, Johanson K, Concha NO, Chan W, Abdel-Meguid SS, Badger AM, Lark MW, Nadeau DP, Suva LJ, Gowen M, Nuttall ME. Potent and selective nonpeptide inhibitors of caspases 3 and 7 inhibit apoptosis and maintain cell functionality. J Biol Chem 2000;275(21):16007–16014. [PubMed: 10821855]
17. Zhou D, Chu W, Rothfuss J, Zeng C, Xu J, Jones L, Welch MJ, Mach RH. Synthesis, radiolabeling, and in vivo evaluation of an 18F-labeled isatin analog for imaging caspase-3 activation in apoptosis. Bioorg Med Chem Lett 2006;16(19):5041–5046. [PubMed: 16891117]
18. Faust A, Wagner S, Law MP, Hermann S, Schnockel U, Keul P, Schober O, Schafers M, Levkau B, Kopka K. The nonpeptidyl caspase binding radioligand (S)-1-(4-(2-[18F]Fluoroethoxy)-benzyl)-5-[1-(2-methoxymethylpyrrolidinyl)s ulfonyl]isatin ([18F]CbR) as potential positron emission tomography-compatible apoptosis imaging agent. Q J Nucl Med Mol Imaging 2007;51(1):67–73. [PubMed: 17372575]
19. Zhou D, Chu W, Chen DL, Wang Q, Reichert DE, Rothfuss JM, D'Avignon A, Welch MJ, Mach RH. [18F] and [11C]N-benzyl-isatin sulfonamide analogues as PET tracers for apoptosis: Synthesis, radiolableing mechanism, and in vivo imaging study of apoptosis in Fas-treated mice using [11C] WC-98. Org Biomol Chem. **Accepted for publication.**
20. Faa G, Ledda-Columbano GM, Ambu R, Congiu T, Coni P, Riva A, Columbano A. An electron microscopic study of apoptosis induced by cycloheximide in rat liver. Liver 1994;14(5):270–278. [PubMed: 7997086]
21. Ledda-Columbano GM, Coni P, Faa G, Manenti G, Columbano A. Rapid induction of apoptosis in rat liver by cycloheximide. Am J Pathol 1992;140(3):545–549. [PubMed: 1546740]
22. Kumar, S. Measurement of caspase activity in cells undergoing apoptosis. In: Brady, HJM., editor. Apoptosis Methods and Protocols. Totowa: Humana Press, Inc.; 2004. p. 19-30.
23. Holm S. A simple sequentially rejective Bonferroni test procedure. Scand Stat Theory Appl 1979;6:65–70.
24. Blankenberg FG, Katsikis PD, Tait JF, Davis RE, Naumovski L, Ohtsuki K, Kopiwoda S, Abrams MJ, Darkes M, Robbins RC, Maecker HT, Strauss HW. In vivo detection and imaging of phosphatidylserine expression during programmed cell death. Proc Natl Acad Sci U S A 1998;95 (11):6349–6354. [PubMed: 9600968]
25. Yagle KJ, Eary JF, Tait JF, Grierson JR, Link JM, Lewellen B, Gibson DF, Krohn KA. Evaluation of 18F-annexin V as a PET imaging agent in an animal model of apoptosis. J Nucl Med 2005;46(4): 658–666. [PubMed: 15809489]
26. Zeng W, Yao ML, Townsend D, Kabalka G, Wall J, Le Puil M, Biggerstaff J, Miao W. Synthesis, biological evaluation and radiochemical labeling of a dansylhydrazone derivative as a potential imaging agent for apoptosis. Bioorg Med Chem Lett 2008;18(12):3573–3577. [PubMed: 18490161]

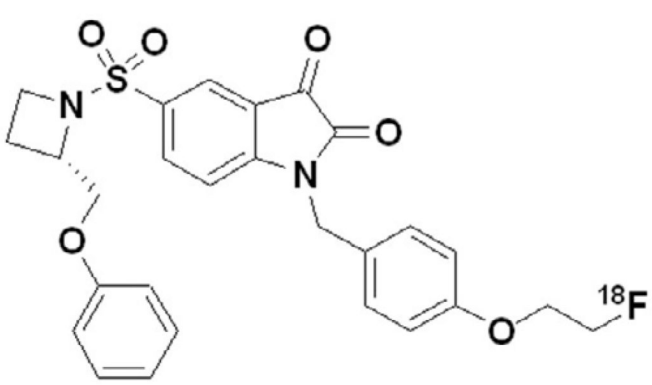

[^{18}F]WC-IV-3

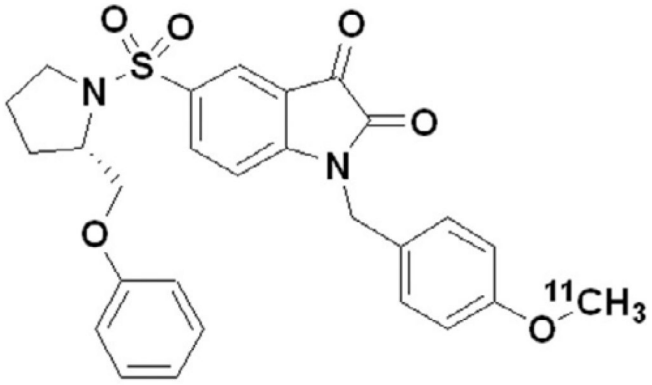

[^{11}C]WC-98

1.
Structures of [^{18}F]WC-IV-3 and [^{11}C]WC-98.

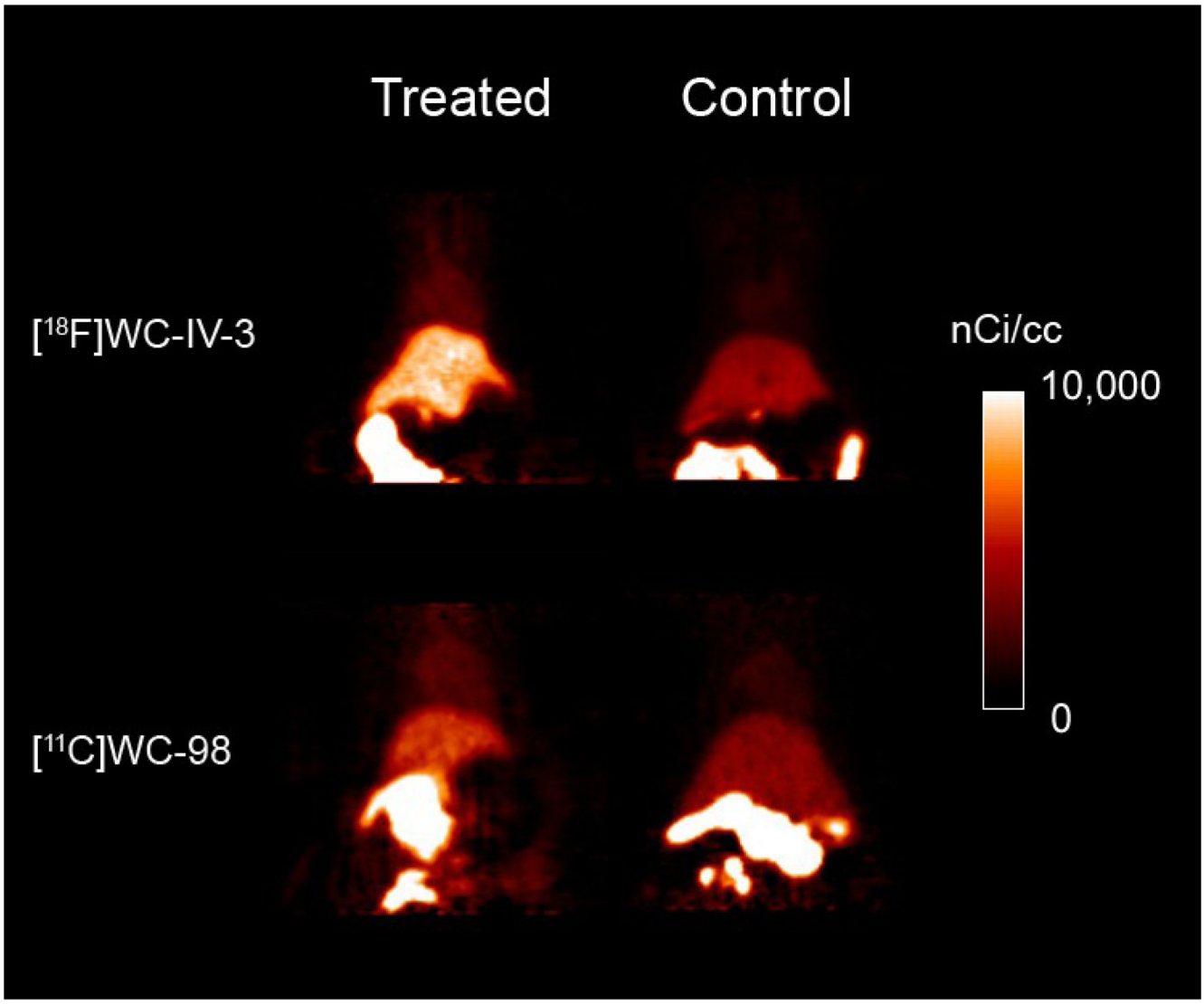

2.

Summed images from a 60-minute dynamic acquisition of rats treated with 5 mg/kg cycloheximide 3 hours prior to injection of ~250 μCi of [^{18}F]WC-IV-3 or ~340 μCi of [^{11}C] WC-98. Rats were imaged while under 1–2% isoflurane anesthesia. There is clearly increased tracer retention in the liver in the treated animals compared with controls; however, the total amount of tracer retained in the liver is clearly higher with [^{18}F]WC-IV-3 than with [^{11}C] WC-98 in this set of imaging studies.

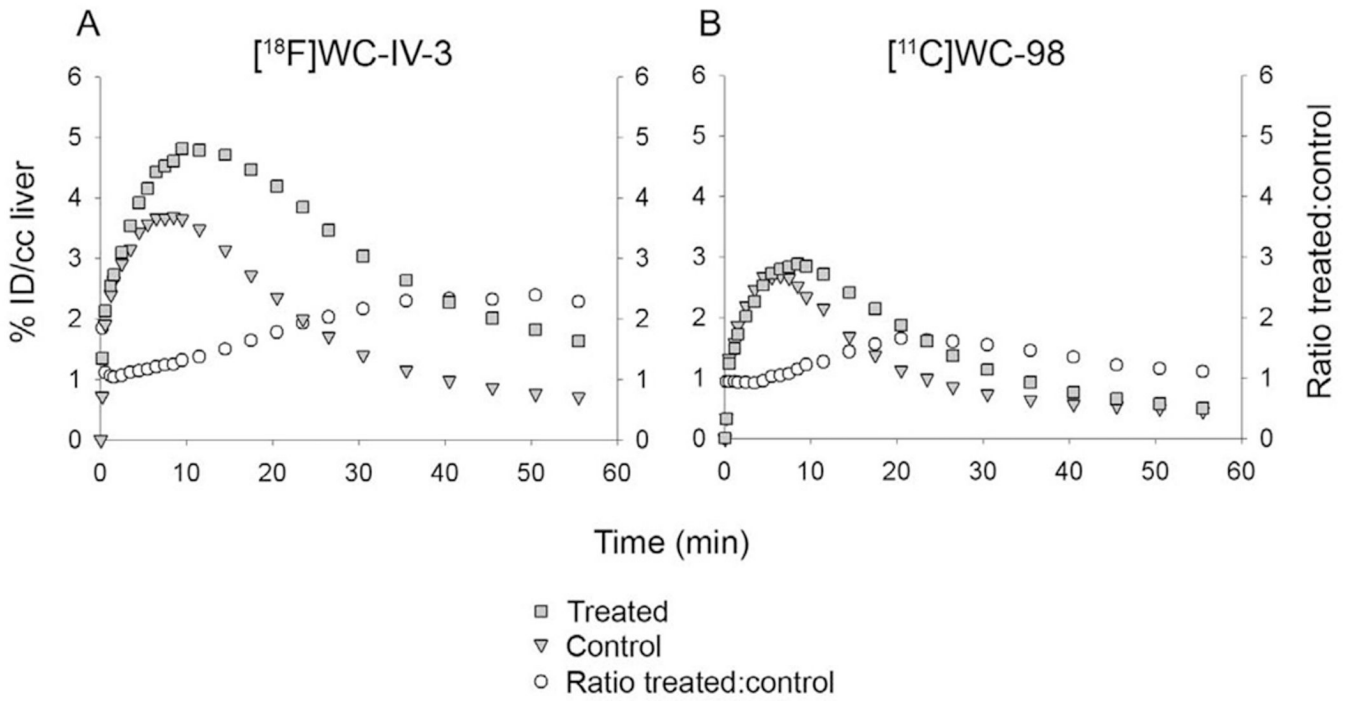

3.

Time-activity curves from the microPET imaging studies shown in Figure 2, obtained by placing volumes of interest over the left lobe of the liver. Retention of [^{18}F]WC-IV-3 in the treated animal persists over the course of the imaging session, whereas [^{11}C]WC-98 washes out over time. %ID/cc liver = % injected dose per cc liver. Ratio treated:control = ratio of activity in treated animal to control animal.

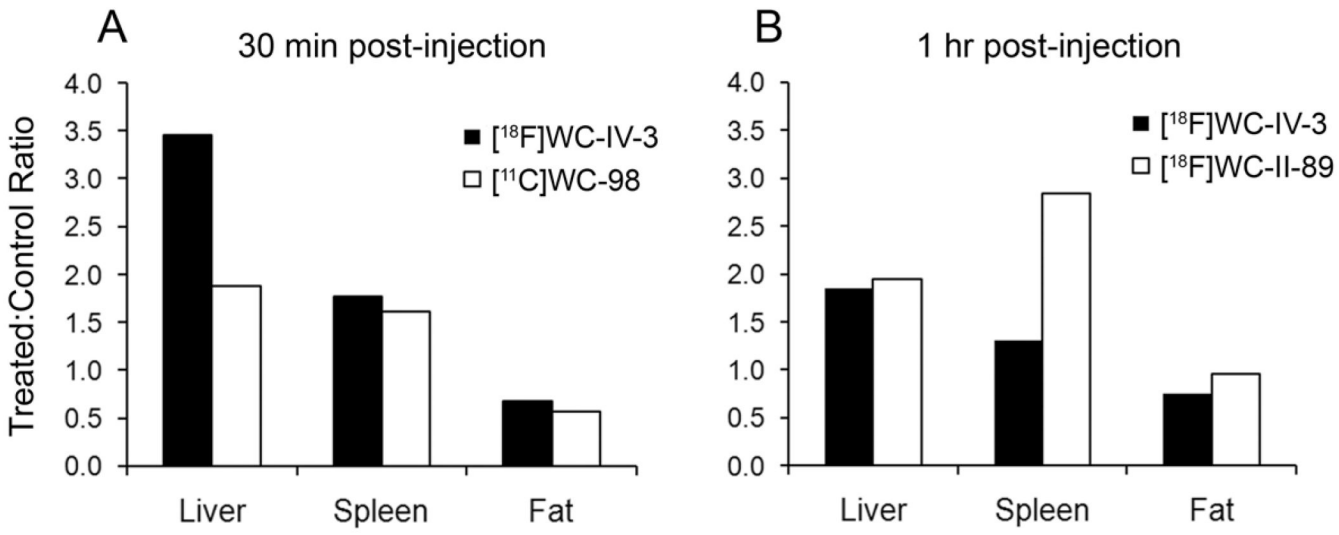

4.

Comparison of relative increase in uptake over control between different tracers. A. At 30 minutes, the increase in uptake of both [^{18}F]WC-IV-3 and [^{11}C]WC-98 is similar in magnitude in the liver, spleen, and fat. B. At 1 hour, the magnitude of increase in uptake of [^{18}F]WC-II-89 is similar to [^{18}F]WC-IV-3 in both liver and fat, but is clearly higher in the spleen.

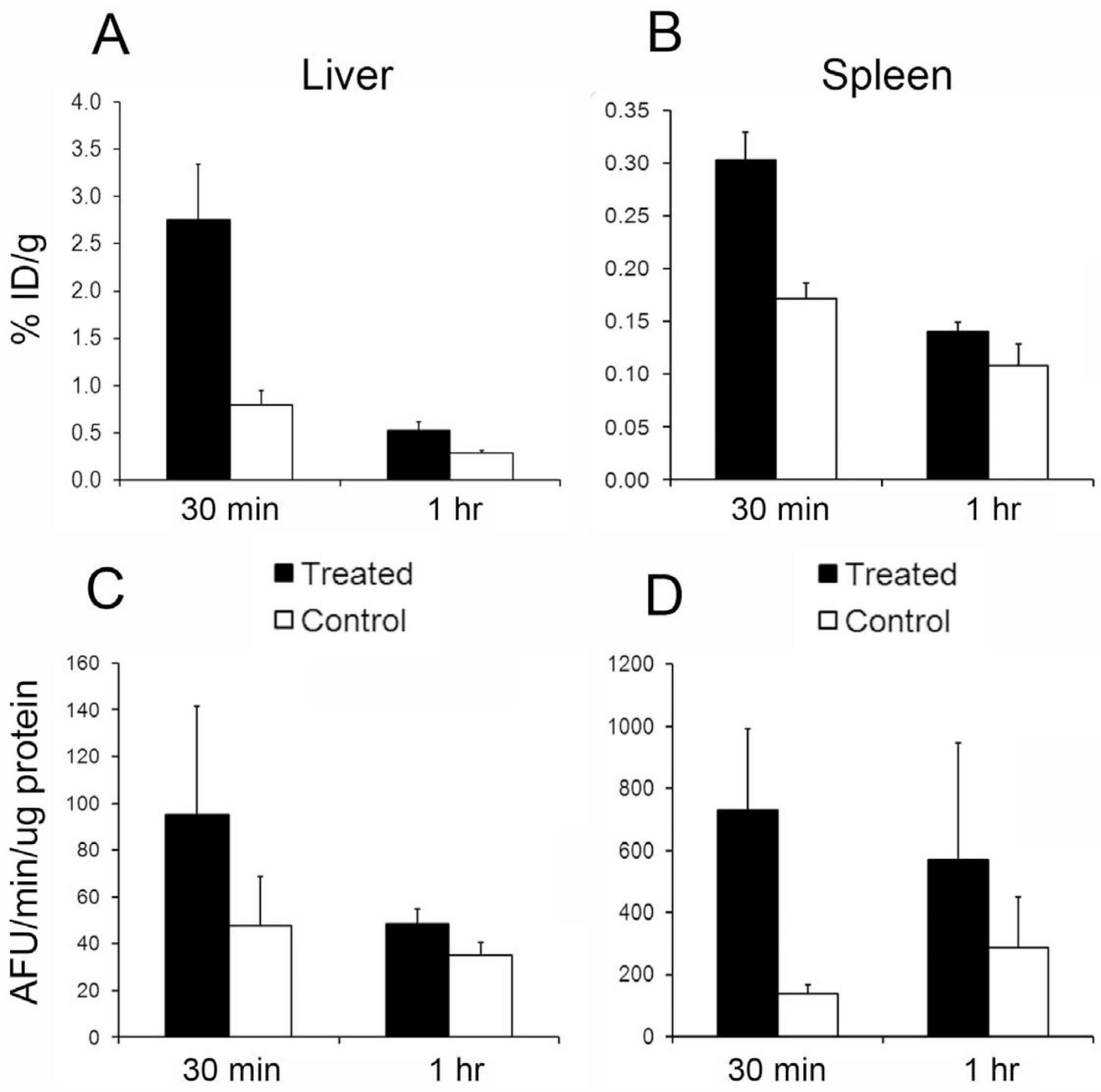

5.

Comparison of levels of [^{18}F]WC-IV-3 uptake in liver and spleen compared to rates of caspase-3 activity measured by fluorometric enzymatic assay of caspase-3 activity. A. [^{18}F] WC-IV-3 uptake in liver at 30 minutes and 1 hour post-tracer injection, with corresponding caspase-3 enzyme activity levels in panel C. Panels B and D illustrate the same information for the spleen. Note that the magnitude of difference in [^{18}F]WC-IV-3 uptake between treated and control at each time point in both organs appears to reflect the magnitude of difference in caspase-3 activity levels. Boxes represent mean, error bars standard deviation.

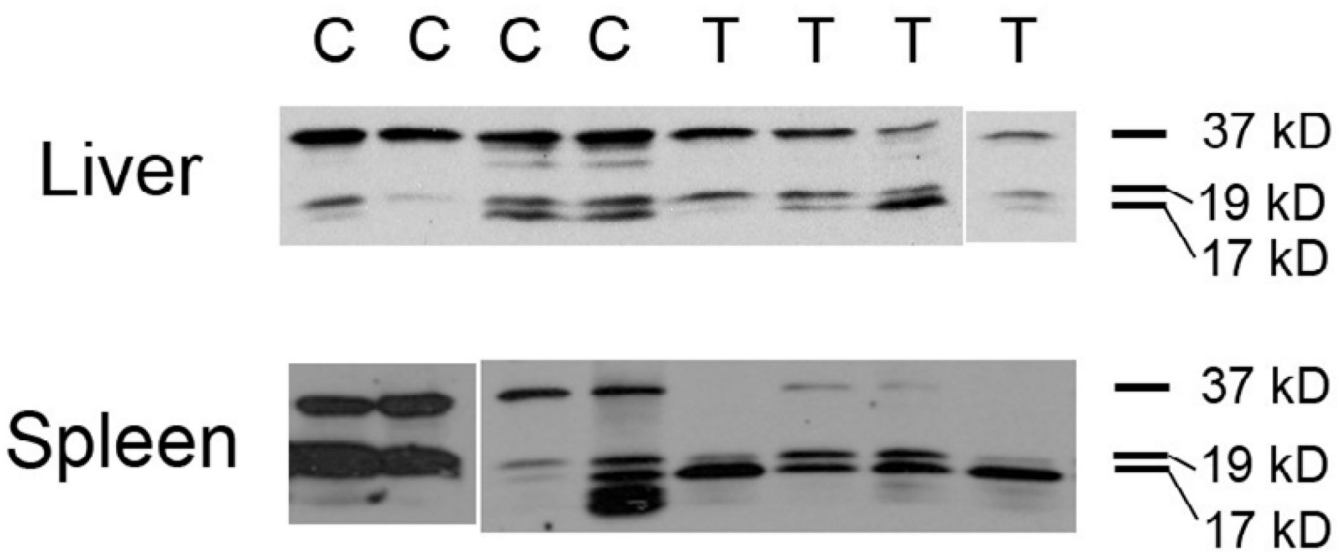

6.

Western blots of liver and spleen samples from the [^{18}F]WC-IV-3 biodistribution study (from animals sacrificed at 30 minutes after tracer injection). Note that, with both liver and spleen, there is loss of the 37 kD procaspase band in the treated (T) animals vs controls (C) with correlating increases in the cleaved caspase-3 bands (17 and 19 kD). There is also variability in the amount of caspase-3 activation in response to the cycloheximide, as noted also with the fluorometric data. In two of the control livers, there was a higher level of cleaved caspase-3 than in the 2 other controls, implying natural variability in baseline levels of apoptosis in the liver.

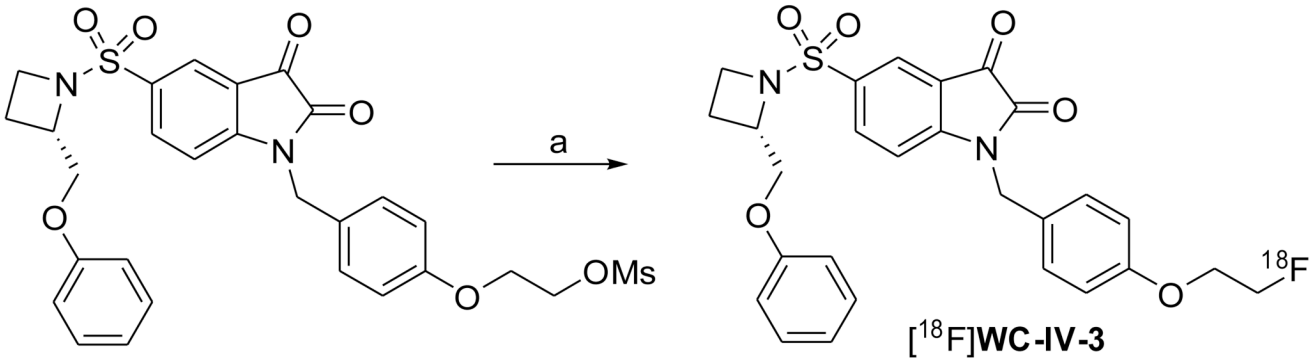

Scheme 1.
(a) 1. $[^{18}F]F^{-}$, K_2CO_3, K_{222}, DMSO, Microwave; 2. 1N HCl, Microwave

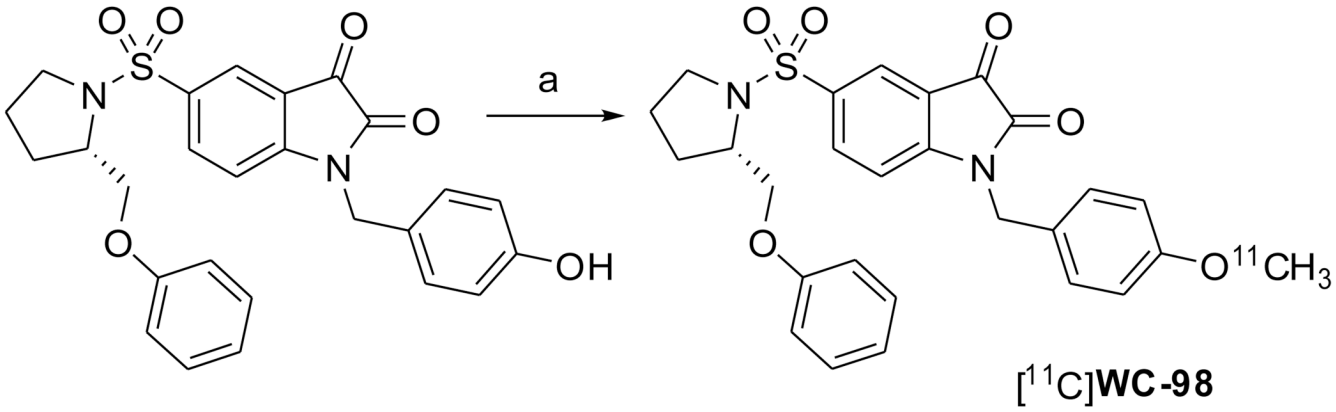

Scheme 2.
(a) 1. Bu_4NOH, CH_3CN; 2.$^{11}CH_3I$, 88°C; 3. 1N HCl, 88°C

Table 1

Inhibition of caspases by [^{18}F]WC-IV-3 and [^{11}C]WC-98.

Compound	IC_{50} (nM)					Log P
	Caspase-1	Caspase-3	Caspase-6	Caspase-7	Caspase-8	
[^{18}F]WC-IV-3	>20,000	8.6 ± 1.0	4930 ± 1240	26.1 ± 1.5	>25,000	3.65 ± 0.51
[^{11}C]WC-98	>20,000	14.5 ± 1.6	>10,000	21.8 ± 3.5	>50,000	3.97 ± 0.43
[^{18}F]WC-II-89	>50,000*	9.7 ± 1.3*	3700 ± 390*	23.5 ± 3.5*	>50,000*	4.19 ± 0.51

*from reference 17.

Table 2

Biodistribution data with [^{18}F]WC-IV-3.

		% ID/g tissue (mean ± SD)		
Organ	**Group***	**5 min**	**30 min**	**1 hour**
Blood	Treated	2.552 ± 0.290	0.207 ± 0.138†	0.123 ± 0.043
	Control	1.658 ± 0.210	0.142 ± 0.011	0.097 ± 0.011
Liver	Treated	3.647 ± 0.389	2.750 ± 0.596†	0.524 ± 0.086†
	Control	3.519 ± 0.187	0.797 ± 0.143	0.284 ± 0.029
Spleen	Treated	1.387 ± 0.132	0.303 ± 0.026†	0.140 ± 0.009
	Control	0.885 ± 0.148	0.171 ± 0.015	0.108 ± 0.021
Muscle	Treated	0.080 ± 0.021	0.140 ± 0.023	0.089 ± 0.011
	Control	0.128 ± 0.028	0.116 ± 0.002	0.066 ± 0.002
Fat	Treated	0.053 ± 0.022	0.091 ± 0.018	0.069 ± 0.001‡
	Control	0.085 ± 0.015	0.135 ± 0.024	0.092 ± 0.008
Heart	Treated	1.163 ± 0.132	0.267 ± 0.027†	0.101 ± 0.009
	Control	0.825 ± 0.090	0.157 ± 0.009	0.087 ± 0.008
Lung	Treated	1.482 ± 0.210	0.358 ± 0.064†	0.136 ± 0.009
	Control	1.148 ± 0.440	0.231 ± 0.020	0.122 ± 0.011
Thymus	Treated	0.330 ± 0.105	0.175 ± 0.014†	0.086 ± 0.004
	Control	0.191 ± 0.037	0.116 ± 0.006	0.075 ± 0.006
Kidney	Treated	1.498 ± 0.239	2.009 ± 0.180†	0.838 ± 0.071
	Control	1.422 ± 0.178	1.427 ± 0.100	0.836 ± 0.102
Brain	Treated	0.106 ± 0.019	0.037 ± 0.007	0.024 ± 0.002
	Control	0.076 ± 0.015	0.029 ± 0.002	0.029 ± 0.003
Bone	Treated	0.547 ± 0.032	0.156 ± 0.019†	0.096 ± 0.004
	Control	0.319 ± 0.029	0.094 ± 0.004	0.115 ± 0.032

*N=4 for all groups except 5 min control and 1 hour treated groups (where N=3 due to exclusion of animals with poor tracer injections).

†$p < 0.05$ when treated compared to control.

‡$p < 0.05$. Note that the level of tracer uptake is higher in the control rather than in the treated group.

%ID/g = % injected dose per gram; SD = standard deviation

Table 3

Biodistribution data with [^{11}C]WC-98

		% ID/g tissue (mean ± SD)	
Organ	**Group**	**5 min***	**30 min****
Blood	Treated	2.328	0.205 ± 0.048
	Control	1.797 ± 0.040	0.148 ± 0.022
Liver	Treated	2.885	1.170 ± 0.085†
	Control	2.533 ± 0.417	0.621 ± 0.041
Spleen	Treated	1.413	0.323 ± 0.091
	Control	0.982 ± 0.088	0.201 ± 0.035
Muscle	Treated	0.088	0.103 ± 0.012
	Control	0.117 ± 0.010	0.108 ± 0.007
Fat	Treated	0.070	0.074 ± 0.020‡
	Control	0.099 ± 0.021	0.130 ± 0.010
Heart	Treated	1.154	0.242 ± 0.048
	Control	0.950 ± 0.020	0.193 ± 0.021
Lung	Treated	1.534	0.294 ± 0.089
	Control	1.181 ± 0.104	0.239 ± 0.026
Thymus	Treated	0.288	0.159 ± 0.022
	Control	0.227 ± 0.061	0.120 ± 0.009

*N=2 for the treated group and N=3 for the control group. Therefore, statistical analysis was not performed. Only the mean is reported for the treated group.

**N=4 in both treated and control groups at 30 min.

†$p < 0.05$ when comparing treated to control. Statistical analysis was applied only to the 30 minute data as the number of animals in each group at 5 minutes, after elimination of animals with bad injections, was too small.

‡$p < 0.05$. Note that the level of tracer uptake is higher in the control rather than in the treated group.

%ID/g = % injected dose per gram; SD = standard deviation